

NONLINEAR OPTICAL PHENOMENA

PACS numbers: 42.65.Dr; 42.65.Ky; 42.70.Nq; 61.46.–w
DOI: 10.1070/QE2010v040n06ABEH014256

Low-threshold anti-Stokes frequency conversion in $Zn_{0.6}Cd_{0.4}S$ microcrystals with adsorbed metal-organic nanoclusters

O.V. Ovchinnikov, M.S. Smirnov, A.N. Latyshev, L.Yu. Leonova,
E.A. Kosyakova, V.G. Klyuev, E.P. Tat'yanina

***Abstract*. We demonstrate the feasibility of low-threshold (10^{-4} to 10^{-2} W cm^{-2}) anti-Stokes conversion of photons in the range 1.72 – 2.00 eV to luminescence at 2.14 – 2.38 eV at temperatures from 77 to 300 K in $Zn_{0.6}Cd_{0.4}S$ crystals with nanoscale complexes of dye molecules and silver subnanoclusters adsorbed on their surface. The spectral characteristics of the centres involved in anti-Stokes frequency conversion indicate that this process in the crystals studied is due to sequential two-photon interband optical transitions. The absorption of a photon by a dye molecule and electron excitation transfer to an adsorbed silver subnanocluster produce a free hole in the valence band. Subsequent photoionisation of the subnanocluster produces a free electron. The last step of the anti-Stokes frequency conversion process is radiative recombination of the electron with a hole localised at an emission centre.**

Keywords: *anti-Stokes frequency conversion, two-photon interband optical transitions, metal-organic subnanoclusters, luminescence.*

1. Introduction

An important issue in designing three-dimensional (3D) optical memory elements, optical switches, power limiters and other devices is the development of materials possessing optical nonlinearity strong enough to ensure low thresholds of the processes involved [1 – 3]. In particular, there is considerable interest in materials that exhibit two-photon-excited anti-Stokes luminescence [4, 5]. Anti-Stokes phosphors include wide-gap semiconductors containing 3D and surface defects [6 – 12], rare-earth-doped crystals [10, 12], semiconductor heterostructures [13 – 15] and systems based on quantum dots [16 – 18] and quantum wells [19, 20]. Most of them, however, have a high anti-Stokes frequency conversion (AFC) threshold: 1 to 10^3 W cm^{-2} [4, 16 – 19]. Lower thresholds (10^{-3} to 10^{-1} W cm^{-2}) can typically be achieved at low temperatures (4.2 – 77 K) [7, 8, 13, 14]. The lowest threshold process (10^{-9} to 10^{-5} W cm^{-2}) is the excitation of sensitised anti-Stokes luminescence (SASL) at low temperatures in silver halide crystals with organic dye molecules or their aggregates adsorbed on the crystal surface [8, 9, 20, 21]. Such heterogeneous systems enable anti-Stokes conversion of photons absorbed by dye molecules (1.7 – 2.0 eV) to luminescence (2.5 – 2.8 eV) [10, 11]. At very low temperatures (2 – 4.2 K), the AFC quantum efficiency is 10^{-3} to 10^{-2}. As pointed out by Ovsyankin and Feofilov [10], the AFC in such materials (like in rare-earth-doped materials [12]) is due to the cooperative summation of the electron excitation energies of two simultaneously excited dye molecules the interaction between which, though weak, is sufficient for this process to take place and for the sum energy to be transferred to the crystal.

Recent work [22, 23] has shown that the efficiency of the AFC process in question can be raised by two orders of magnitude or more by creating, along with organic dye molecules, Ag_n ($n = 1, 2, \ldots$) silver subnanoclusters on the surface of silver halide crystals. This unusual nonlinear optical effect is of interest because of its low threshold. In particular, such model systems were used to demonstrate conceptual feasibility of low-threshold power limiting (0.1 W cm^{-2}) for cw 660-nm light [5, 24]. Silver halide crystals are, however, of limited utility for AFC in practical applications because of their high photochemical activity under optical excitation. The conditions for the development of such effects in other crystals that exhibit efficient luminescence at room temperature are not yet clear. For example, anti-Stokes frequency conversion at high excitation densities was detected in $Zn_xCd_{1-x}S$ solid solutions doped with metallic impurities (Pb, Fe, Cu and others) [6 – 9].

The results presented in this paper demonstrate the feasibility of AFC at 300 K and excitation intensities from 10^{-4} to 10^{-2} W cm^{-2} in $Zn_{0.6}Cd_{0.4}S$ crystals with dye molecules and silver subnanoclusters adsorbed on their surface. We used dyes of the thiazine (methylene blue), carbocyanine (1,1′-diethyl-2,2′-quinocyanine 3,3′-di(γ-sulphopropyl)-9-ethyl-4,5-benzo-4′,5′-[4″5″-dimethyleno(2″3″)]-thiathiazolocarbocyaninebetaine salt) and triphenylmethane (malachite green) series (D1, D2 and D3, respectively). These dyes are capable of forming various aggregates. D1 and D2 typically form H- and J-aggregates, respectively, whereas D3 has no tendency to aggregate [25, 26]. Monomers and aggregates of these dyes have absorption bands in the range 600 – 730 nm. Note that the photon energy in this range slightly exceeds half the band gap of $Zn_{0.6}Cd_{0.4}S$ evaluated by the additivity rule (3.25 – 3.30 eV). This relationship is a necessary condition for anti-Stokes lumi-

O.V. Ovchinnikov, M.S. Smirnov, A.N. Latyshev, L.Yu. Leonova, E.A. Kosyakova, V.G. Klyuev, E.P. Tat'yanina Voronezh State University, Universitetskaya pl. 1, 394006 Voronezh, Russia;
e-mail: opt@phys.vsu.ru, leonova@phys.vsu.ru

Received 17 November 2009
Kvantovaya Elektronika **40** (6) 490 – 494 (2010)
Translated by O.M. Tsarev

nescence excitation, like in the case of the SASL in silver halide crystals [23].

2. Characterisation techniques and apparatus

We studied high-purity $Zn_{0.6}Cd_{0.4}S$ microcrystals (0.7–1.3 μm) grown at the Institute of Solid State Physics, Russian Academy of Sciences (Chernogolovka). X-ray diffraction examination (DRON-3 diffractometer) showed that the only phase in the crystals was a substitutional solid solution. To enhance the luminescence of the $Zn_{0.6}Cd_{0.4}S$ microcrystals, they were annealed for 1 h at 650 – 700 K in a nitrogen atmosphere and in the presence of NaCl as a flux (10^{-2} mol NaCl per mole of $Zn_{0.6}Cd_{0.4}S$) by a standard technique [27]. This ensured a factor of 150 – 200 increase in the quantum yield of $Zn_{0.6}Cd_{0.4}S$ luminescence in the band with $\lambda_{max} = 570$ nm under UV excitation at 365 nm, which had a significant effect on AFC efficiency. When the surface of the $Zn_{0.6}Cd_{0.4}S$ crystals was free of dye molecules and silver subnanoclusters, no SASL was detected.

Adsorptions were performed by immersing the $Zn_{0.6}Cd_{0.4}S$ crystals in ethanolic solutions of D1, D2 or D3 of controlled concentration, followed by drying. The mole fraction of the dyes in the solutions was varied from 10^{-6} to 10^{-2}. A number of samples had, in addition to dye molecules, silver subnanoclusters on their surface. To this end, the microcrystals were treated with aqueous solutions of $AgNO_3$ (mole fraction from 10^{-8} to 10^{-5}).

AFC processes in the $Zn_{0.6}Cd_{0.4}S$ crystals with dye molecules and silver subnanoclusters adsorbed on their surface were studied by luminescence and absorption spectroscopies. The spectral range where radiation absorbed by surface impurity centres was converted to $Zn_{0.6}Cd_{0.4}S$ photoluminescence was determined from SASL excitation spectra. In addition, the anti-Stokes luminescence spectrum taken at a fixed excitation frequency was compared to the spectrum obtained under UV excitation in the region of the fundamental absorption band. In this way, we assessed the nature of the centres responsible for the luminescence under Stokes and anti-Stokes excitation. Information about two-photon interband optical transitions leading to SASL in $Zn_{0.6}Cd_{0.4}S$ with dye molecules and few-atom silver subnanoclusters adsorbed on its surface was gained from SASL excitation spectra. Comparison of these with the absorption spectra of the adsorbed dye molecules provided insight into the role of the dye molecules in the two-photon AFC process.

Changes in the spectra of the deep impurity states resulting from the adsorption of dye molecules and silver subnanoclusters on the $Zn_{0.6}Cd_{0.4}S$ crystals were assessed by analysing the IR-stimulated luminescence burst after photoexcitation of the sample [28]. Such data were needed to construct a model of the effect in question. The photostimulated luminescence burst (PSLB) was measured in the main recombination luminescence band of the $Zn_{0.6}Cd_{0.4}S$ crystals, centred at 570 nm, using IR radiation that ionised the deep electronic states related to the adsorbate. The PSLB energy measured when IR radiation ionises deep electronic states is proportional to their density [28].

The luminescence parameters of our samples were measured using an automatic spectrometer system [29]. To excite Stokes luminescence and produce a PSLB, we used the UV radiation from an HPL-H77GV1BT-V1 diode ($\lambda = 380$ nm) with a photon flux density of 10^{15} cm^{-2} s^{-1}. Luminescence spectra and PSLB signals were measured using an MDR-23 grating monochromator (LOMO, Russia), a photon-counting detector (R928P photomultiplier, Hamamatsu, Japan) placed at the exit slit of the MDR-23 and a C4900-51 power supply (Hamamatsu, Japan). SASL excitation spectra were obtained using a KGM-36-400 halogen lamp and an MDR-4 grating monochromator (LOMO, Russia). The monochromator slit width was adjusted so that the excitation source bandwidth was 0.05 eV, and the radiant flux incident on the sample for SASL excitation was maintained constant throughout the spectral range studied (1.60 – 2.05 eV). To this end, we varied the current through the tungsten filament of the halogen lamp, whose output was monitored with an IMO-2M optical power meter. The SASL excitation intensity could be varied from 10^{-4} to 10^{-2} W cm^{-2} throughout the spectral range studied. A computer-interfaced system was used to control the SASL excitation intensity and record photomultiplier pulses.

Absorption data for the adsorbed dye molecules were extracted from diffuse reflection spectra taken on a Shimadzu 210 double-beam UV spectrophotometer (Japan) equipped with an integrating sphere (1-nm resolution in the range 400 – 800 nm).

3. Results and discussion

At 300 K, photon energies from 1.60 to 2.00 eV and incident power densities from 10^{-3} to 10^{-2} W cm^{-2}, the $Zn_{0.6}Cd_{0.4}S$ crystals having D1-D3 molecules on their surface (mole fraction from 10^{-5} to 10^{-4}) exhibited AFC [Fig. 1, spectra (*1*–*3*)] to luminescence centred around 2.20 eV [spectra (*4*)]. The SASL excitation spectra of those samples were identical in position and similar in shape to the absorption spectra of the adsorbed dye molecules [spectra (*1′*–*3′*)]. The maximum in the excitation spectrum of the $Zn_{0.6}Cd_{0.4}S$ crystals having D1 molecules on their surface (1.82 – 1.88 eV) seems to arise from light absorption by D1 monomers, and the shoulder at 1.97 – 2.00 eV is due to a part of the absorption band of D1 H-aggregates [25, 26] [spectrum (*1*)]. The complex structure of spectrum *2* is attributable to the participation of both D2 monomers and D2 J-aggregates in SASL excitation. Indeed, photon energies between 1.88 and 2.00 eV correspond to the absorption range of adsorbed D2 monomers, and those between 1.77 and 1.80 eV correspond to the absorption range of D2 J-aggregates [spectrum (*2′*)]. In the case of D3, which forms no aggregates when adsorbed on crystal surfaces [25], there was only one, elementary SASL excitation band [spectrum (*3*)], identical in position to the absorption band of adsorbed malachite green molecules [spectrum (*3′*)]. The above results can be interpreted in terms of a cooperative model of SASL, similar to the model proposed by Ovsyankin and Feofilov [10] for silver halides.

The frequencies obtained under anti-Stokes excitation in the absorption range of adsorbed D1-D3 molecules coincide with those in their luminescence spectra under UV excitation in the region of their fundamental absorption band [Fig. 1, spectra (*4*)]. The spectra have the form of a band centred at 2.18 ± 0.05 eV, with a full width at half maximum of ~ 0.22 eV [spectra (*4*)]. This suggests that the radiative recombination centres responsible for SASL and conventional intrinsic recombination luminescence in the $Zn_{0.6}Cd_{0.4}S$ microcrystals are of the same nature.

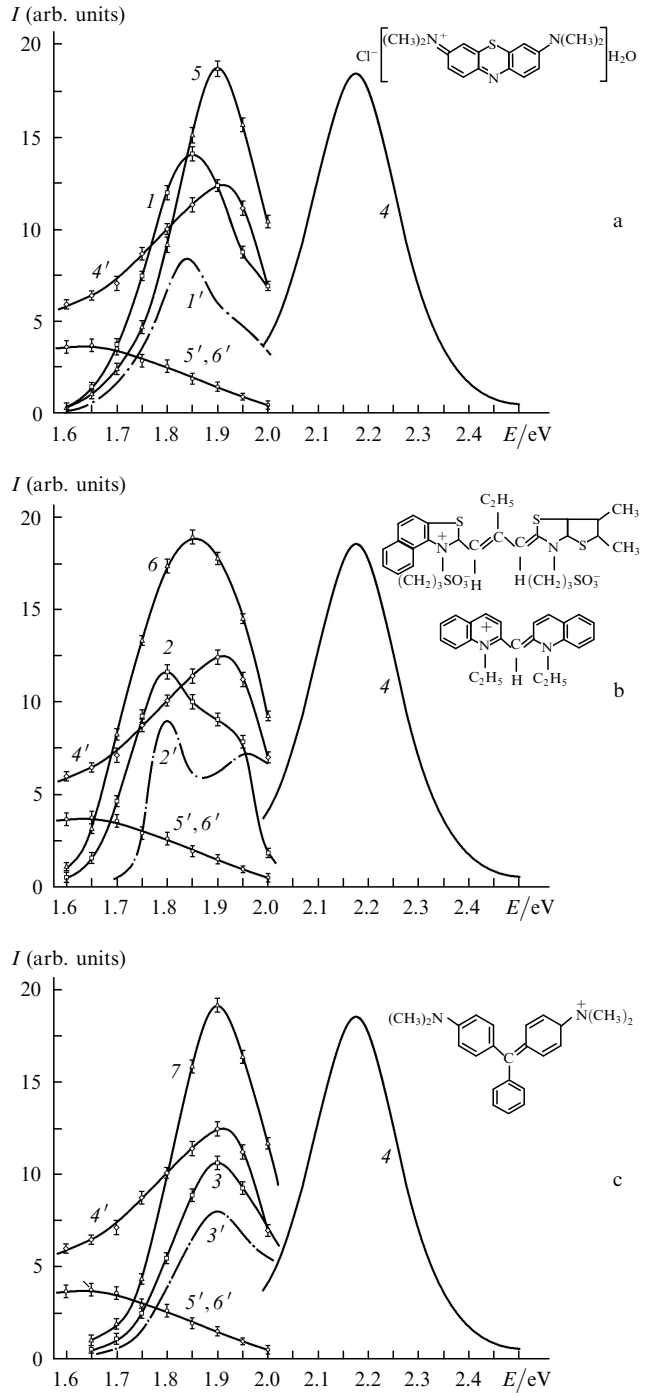

Figure 1. AFC in $Zn_{0.6}Cd_{0.4}S$ microcrystals with silver subnanoclusters and (a) D1, (b) D2 and (c) D3 molecules adsorbed on their surface: (*1*–*3*) SASL excitation spectra of the crystals having dye molecules on their surface (mole fraction, 10^{-4}); (*4*) SASL spectra; (*1′*–*3′*) absorption spectra of these crystals; (*5*–*7*) SASL spectra of the crystals having dye molecules and Ag_n subnanoclusters (mole fraction, 10^{-7}) on their surface; (*4′*–*6′*) PSLB spectra of the samples having dye molecules and silver subnanoclusters with a mole fraction of (*4′*) 10^{-7}, (*5′*) 10^{-6} and (*6′*) 10^{-8}

Another important result is that the AFC efficiency depends on the ultralow concentration of the silver-containing solution (mole fraction from 10^{-8} to 10^{-6}). Adsorption of silver subnanoclusters in this concentration range may produce 10^9 to 10^{11} Ag_n ($n = 1, 2, \ldots$) subnanoclusters per square centimetre of the $Zn_{0.6}Cd_{0.4}S$ surface. The most interesting information is provided by the SASL excitation spectra of the $Zn_{0.6}Cd_{0.4}S$ microcrystals that had D1-D3 molecules on their surface and were then treated with silver-containing solutions at a 10^{-7} mole fraction of silver [Fig. 1, spectra (*5*–*7*)]. This treatment influenced not only the intensity but also the position of the SASL excitation band. The excitation band of the $Zn_{0.6}Cd_{0.4}S$ samples having D1 and D2 molecules and silver atoms and subnanoclusters adsorbed on their surface was shifted to 1.85-1.91 eV [spectra (*5*, *6*)]. An important point is that those samples had an increased anti-Stokes emission intensity and showed AFC at excitation intensities as low as 10^{-4} to 10^{-3} W cm^{-2}. Note that, at a 10^{-8} or 10^{-5} mole fraction of $AgNO_3$, the SASL intensity was lower compared to the samples that had only dye molecules on their surface, but the spectra of those samples were similar in shape to spectra (*1*–*3*) in Fig. 1.

To rationalise these findings, we analysed the changes in the spectra of deep electronic states using PSLB data [Fig. 1, spectra (*4′*, *5′*)]. Note first of all that, according to the PSLB spectra, D1-D3 adsorption on $Zn_{0.6}Cd_{0.4}S$ produces no traps 1.50–2.00 eV below the conduction band bottom. The fact that, at a given concentration of silver subnanoclusters, we obtained similar PSLB spectra with different dyes indicates that the dyes do not contribute to the luminescence burst. The adsorption of silver ions on $Zn_{0.6}Cd_{0.4}S$ from $AgNO_3$ solutions, with or without dye molecules, yields similar spectra [Fig. 1, spectra (*4′*, *5′*)]. At a 10^{-7} mole fraction of silver ions, the spectrum of deep electronic states shows a maximum at photon energies from 1.80 to 1.90 eV [spectra (*4′*)]. The maximum overlaps with the SASL band [spectra (*5*–*7*)] and is close in position to the absorption band of adsorbed D1–D3 molecules [spectra (*1′*–*3′*)]. This leads to an increase in AFC efficiency [spectra (*5*–*7*)]. At the same time, reducing the mole fraction of silver by an order of magnitude (to 10^{-8}) or increasing it to 10^{-6} or 10^{-5} produces no maximum at 1.80-1.90 eV in the spectrum of deep electronic states [spectra (*5′*)]. At the lowest concentrations, the spectrum of deep electronic states has no maximum at all, which is probably due to both the low surface density of adsorbed species and the insufficient sensitivity of the method under consideration. In contrast, at a mole fraction from 10^{-6} to 10^{-5}, a maximum emerges in the range 1.40–1.70 eV. This seems to be due to the formation of increasingly larger silver subnanoclusters, whose optical properties are unsuitable for the excitation of two-photon interband optical transitions at photon energies from 1.80 to 2.00 eV.

Thus, the observed behaviour of the SASL excitation and PSLB spectra indicates that AFC involves not only organic dye molecules but also silver subnanoclusters with photoionisation energies close to the peak absorption energies in the spectra of D1–D3. The presence of silver atoms and few-atom silver subnanoclusters, along with D1–D3 molecules, on the surface of the $Zn_{0.6}Cd_{0.4}S$ microcrystals has a significant effect on the AFC process. The changes in the density of deep electron traps evidenced by the PSLB data confirm that the traps are related to the silver subnanoclusters, and the correlation between the peak positions in the PSLB and SASL excitation spectra at a mole fraction of subnanoclusters from 10^{-7} to 10^{-6} (in the range 1.80–1.90 eV) suggests that the clusters are involved in anti-Stokes emission excitation. D1–D3 molecules influence SASL as evidenced by the fact that no AFC occurs

without dyes. Moreover, the AFC efficiency reaches a maximum when the adsorbed dye molecules are similar in spectral characteristics (within 0.10 – 0.15 eV) to the silver subnanoclusters. When the surface density of silver subnanoclusters becomes high enough for the formation of subnanoclusters larger than those involved in AFC, with energy states in the range 1.60 – 1.70 eV, the anti-Stokes emission intensity decreases. Thus, the centres responsible for two-photon AFC are composed of both dye molecules and silver subnanoclusters. These results shed light on the general nature of the effect under discussion and the additional sensitisation of anti-Stokes luminescence in AgCl(I) crystals as a result of a low-temperature photostimulated process [22, 23].

Consequently, with increasing surface density of silver subnanoclusters on $Zn_{0.6}Cd_{0.4}S$, the cooperative summation of the electron excitation energies of two simultaneously excited dye molecules spaced in the order of one Forster radius apart gradually gives way to another, more effective mechanism of two-photon AFC. Its key point is that, when there is no excitation (and no free holes nearby), adsorbed silver subnanoclusters, acting as deep electron traps, are capable of holding electrons for a time much longer than the excited state lifetime of the dye molecule. The adsorbed dye molecules, strongly absorbing in the SASL excitation range, raise the efficiency of electron transitions from the valence band to levels of the adsorbed silver subnanoclusters through electron excitation transfer (Fig. 2). At the same time, optical transitions from the levels of the adsorbed silver subnanoclusters to the conduction band may be caused by prolonged long-wavelength excitation. The feasibility of such transitions is evidenced by the present PSLB data. For this reason, the SASL excitation probability may be higher in the case under consideration. As a result, the two-photon AFC process involves the following successive steps: absorption of a photon by a dye molecule, transfer of the resultant electron excitation to a nearby silver subnanocluster and Ag_n photoionisation by another photon (Fig. 2). The first step assumes at least van der Waals interaction in the silver subnanocluster-dye molecule system. The resultant hole in the valence band is then localised at an emission centre. The photoionisation of the silver subnanocluster by another photon produces a free electron in the conduction band, which then recombines with the ionised emission centre. This process can be represented by the following scheme:

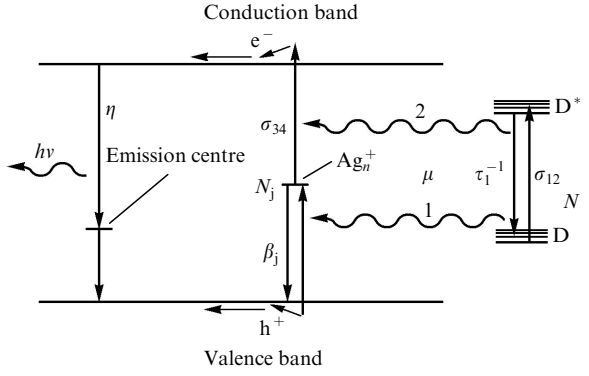

Figure 2. Schematic of low-threshold AFC in $Zn_{0.6}Cd_{0.4}S$ microcrystals with metal-organic nanostructures adsorbed on their surface.

$$Zn_{0.6}Cd_{0.4}S + Ag_n^+ + D + 2h\nu \rightarrow Zn_{0.6}Cd_{0.4}S + Ag_n^+ + D^* + h\nu \rightarrow Zn_{0.6}Cd_{0.4}S^{h^+} + Ag_n^0 + D + h\nu \rightarrow Zn_{0.6}Cd_{0.4}S^{h^+e^-} + Ag_n^+ + D \rightarrow Zn_{0.6}Cd_{0.4}S + Ag_n^+ + D + h\nu_{lum},$$

where D stands for a dye molecule.

Analysis of AFC kinetics in terms of this scheme gives the following expression for the SASL intensity:

$$J_{SASL} = \eta \frac{J^2\sigma_{12}\sigma_{34}N_j\mu N}{\sigma_{12}JN\mu + (\sigma_{34}J + \beta_j)(\tau_1^{-1} + N_j\mu)}.$$

Here, J is the excitation intensity; N_j and N are the surface densities of adsorbed metal subnanoclusters and dye molecules, respectively; μ is the rate constant of electron excitation transfer from dye molecules to Ag_n^+; β_j is the probability that an electron at level j recombines with a hole in the valence band; σ_{12} is the effective absorption cross section of the dye molecule; σ_{34} is the effective photoionisation cross section of Ag_n^+; τ_1 is the excited state lifetime of the dye molecule; and η is the luminescence quantum yield in the scheme under consideration.

It follows from this relation that the SASL excitation spectrum generally has a complex structure and depends on both the absorption spectrum of the adsorbed molecules and the photoionisation spectrum of the adsorbed silver subnanoclusters. Moreover, the increase in N_j with the formation of silver subnanoclusters makes an appreciable contribution to the SASL intensity. Electron excitation transfer from a dye molecule to a silver subnanocluster may, in principle, cause an electron transition both from the valence band to a local level (process 1) and from a local level to the conduction band (process 2) (Fig. 2). However, the weak effect of the surface density of silver subnanoclusters on the PSLB signal in our samples (in the range detectable by this method) suggests that process 2 in Fig. 2 is unlikely.

4. Conclusions

The present results demonstrate the feasibility of low-threshold (10^{-4} to 10^{-2} W cm^{-2}) anti-Stokes conversion of photons in the range 1.72 – 2.00 eV to luminescence at 2.14 – 2.38 eV in $Zn_{0.6}Cd_{0.4}S$ crystals having dye molecules and silver subnanoclusters adsorbed on their surface. In such materials, low-threshold AFC can be achieved at room temperature owing to two-photon interband optical transitions in the adsorbed nanoscale complexes of dye molecules and silver subnanoclusters. Two-photon interband optical transitions are shown to occur sequentially, with electron excitation transfer from dye molecules to silver subnanoclusters adsorbed on the $Zn_{0.6}Cd_{0.4}S$ surface, which produce deep local states in the band gap, with photoionisation energies from 1.80 to 1.90 eV. The AFC quantum efficiency estimated from experimental data with allowance for the quantum yield of radiative recombination and the luminescence loss in the case of room-temperature detection is 10^{-4} to 10^{-3} at an excitation intensity of 10^{-2} W cm^{-2}. Blocking the nonradiative recombination channels in the crystals is anticipated to increase the quantum efficiency of the AFC process.

Acknowledgements. This work was supported by the Russian Foundation for Basic Research (Grant No. 08-02-00744).

References

1. Ban D. et al. *J. Appl. Phys.*, **96**, 5243 (2004).
2. Akimov D.A., Zheltikov A.M., Koroteev N.I. *Laser. Phys.*, **7**, 1242 (1997).
3. Potasek M., Kim S., Melaughlin D. *J. Nonlinear Opt. Physics Mat.*, **9**, 343 (2000).
4. Akimov D.A. *Kvantovaya Elektron.*, **23**, 871 (1996) [*Quantum Electron.*, **26**, 848 (1996)].
5. Smirnov M.S. et al. *Opt. Zh.*, **76**, 68 (2009).
6. Brown M.R. et al. *J. Luminesc.*, **1/2**, 78 (1970).
7. Carlone C., Beliveau A., Rowell N.L. *J. Luminesc.*, **47**, 303 (1991).
8. Ivanov V.Yu. et al. *Phys. Rev. B*, **56**, 4696 (1996).
9. Chen W. *Phys. Rev. B*, **64**, 041202 (2001).
10. Ovsyankin V.V., Feofilov P.P. *Pis'ma Zh. Eksp. Teor. Fiz.*, **14**, 548 (1971).
11. Hediger H., Junod P., Steiger R. *J. Luminesc.*, **24/25**, 881 (1981).
12. Ovsyankin V.V., Feofilov P.P. *Pis'ma Zh. Eksp. Teor. Fiz.*, **4**, 471 (1966).
13. Heimbrodt W. et al. *Phys. Rev. B*, **60**, R16326 (1999).
14. Cho Y.H. et al. *Phys. Rev. B*, **56**, R4375 (1997).
15. Seidel W. et al. *Phys. Rev. Lett.*, **73**, 2356 (1994).
16. Kammerer C. et al. *Phys. Rev. Lett.*, **87**, 27401 (2001).
17. Ignatiev I.V. et al. *Phys. Rev. B*, **60**, R14001 (1999).
18. Wang X. et al. *Phys. Rev. B*, **68**, 125318 (2003).
19. Vagos P. *Phys. Rev. Lett.*, **70**, 1018 (1993).
20. Driessen F.A.J.M. et al. *Phys. Rev. B*, **64**, R5263 (2001).
21. Dexter D.L. *J. Chem. Phys.*, **21**, 835 (1953).
22. Ievlev V.M. et al. *Dokl. Akad. Nauk*, **409**, 756 (2006).
23. Ovchinnikov O.V. et al. *Opt. Spektrosk.*, **103**, 497 (2007).
24. Latyshev A.N. et al., RF Patent No. 2 359 299, 16.10.07.
25. Terenin A.N. *Fotonika molekul krasitelei i rodstvennykh organicheskikh soedinenii* (Photonics of Dye Molecules and Related Organic Compounds) (Leningrad: Nauka, 1967).
26. Shapiro B.I. *Teoreticheskie nachala fotograficheskogo protsessa* (Theoretical Principles of the Photographic Process) (Moscow: Editorial, 2000).
27. Aven M., Prener J.S. (Eds) *Physics and Chemistry of II–VI Compounds* (Amsterdam: North-Holland, 1967; Moscow: Mir, 1970).
28. Klyuev V.G., Latyshev A.N. *J. Inf. Rec.*, **23**, 295 (1996).
29. Latyshev A.N. et al. *Prib. Tekh. Eksp.*, **6**, 119 (2004).